Polyelectrolyte brushes: Counterion distribution and complexation properties

Y. Tran,[1] P. Auroy,[1,*] L-T. Lee,[2] and M. Stamm[3]
[1]*Physico-Chimie Curie, UMR 168 du CNRS, Institut Curie, 11 rue Pierre et Marie Curie, 75231 Paris Cedex 05, France*
[2]*Laboratoire Léon Brillouin, CEA-CNRS, CE Saclay, 91191 Gif-Sur-Yvette Cedex, France*
[3]*Max Planck-Institut für Polymerforschung, Postfach 3148, Ackermannweg 10, D-55021 Mainz, Germany*
(Received 24 March 1999)

The structure of dense grafted polyelectrolyte layers has been studied with a combination of neutron reflectivity and infrared spectroscopy techniques. The polyelectrolyte brushes were made of poly(styrene sulfonate) neutralized by different counterions. Small counterions are distributed throughout the brush in order to ensure a highly local electroneutrality. In addition, they can be readily exchanged with other small ions. On the other hand, macromolecular counterions (as well as some proteins) are irreversibly trapped by the brush, but are located outside the grafted layer and cannot reach the surface. [S1063-651X(99)14311-3]

PACS number(s): 68.45.Ws, 61.12.Ex, 61.25.Hq, 82.65.−i

I. INTRODUCTION

Polyelectrolyte brushes [1] are polymer interfaces where the (charged) macromolecules are attached by one end to a surface (cf. Fig. 1) which can be solid (like a glass plate) or fluid (like a vesicle membrane). These charged polymer brushes are thought to be a model of the external envelope of some microorganisms: some viruses or bacteria [2] are surrounded by a kind of capsule which in general is a virulence factor. The reason for this increased pathogenicity is thought to be related to the antiadsorption properties of this external (usually negatively) charged polymer layer: in particular, it should prevent protein adsorption and thus these pathogens would escape more easily recognition by the immune system.

For a similar reason, these polyelectrolyte brushes attract a lot of interest in colloid and material science: they could be used to protect surfaces from the adhesion of undesired materials (proteins or platelets on prostheses or catheters, algae on aquarium windows, etc.). They could also improve the stability of many aqueous dispersions (by a self-avoiding mechanism), especially at moderate and high ionic strength where the ubiquitous van der Waals attraction induces flocculation of the dispersions. Polyelectrolytes are currently used in many applications to modify the surface of aqueous colloids, but usually, the polymer chains are bound to the grains by adsorption: the links (of moderate strength, of the order of a few kT's) are randomly distributed along the backbone. This makes two important differences with polyelectrolyte brushes: first, the amount of polymer per unit area is much less (of the order of 1 mg/m^2, typically 10 times less) and, second, the polymer chains can be displaced by other charged molecules (like surfactants). This can result in hazardous complications.

However, since these adsorbed layers are easily prepared, they have been extensively studied. For instance, the adsorption kinetics [3,4] and the density profile [5] at a solid liquid interface have been determined. The effect of salt has also been considered; in particular, it has been shown that the amount of adsorbed poly(styrene sulfonate sodium salt) (PSSNa) on various surfaces is very small in pure water, but increases upon the addition of salt either in the case of a monolayer [6] or when multilayers (of alternating sign) [7,8] are built. In contrast, polyelectrolyte brushes have been studied mostly theoretically [1,9–11]; very few experimental papers deal with these systems despite their appealing features [12–16].

In this paper, we show that polyelectrolyte brushes can be permeable to small ions, but are an impenetrable barrier for polymers, as long as their molecular weight is high enough. Polymer of opposite charge can bind strongly to the external border of the polyelectrolyte brush, but the complex so formed exhibits remarkable antiadsorption properties.

II. SYNTHESIS OF POLYELECTROLYTE BRUSHES

We followed the same strategy as in Ref. [14]: neutral poly(styrene) (PS) chains were first grafted, then converted to polyelectrolytes by an *in situ* sulfonation reaction. Instead of a porous medium, we used silicon blocks as subtrates. This allowed us to control the chemical modifications of the interfaces at all the different stages of the sample preparation using infrared spectroscopy in attenuated total reflection (IR-

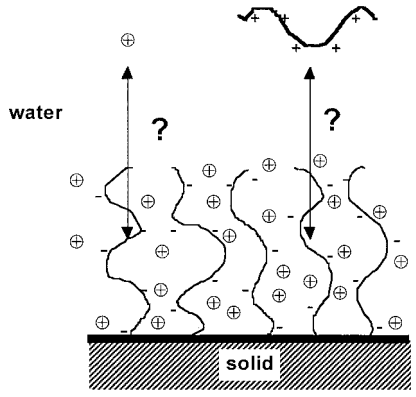

FIG. 1. Schematic view of a polyelectrolyte brush and its influence on the traffic of charged objects between the bulk and the surface. Typical thickness of the polyelectrolyte brush is 500 Å and typical distance between grafting points is 20 Å.

*Author to whom correspondence should be addressed.

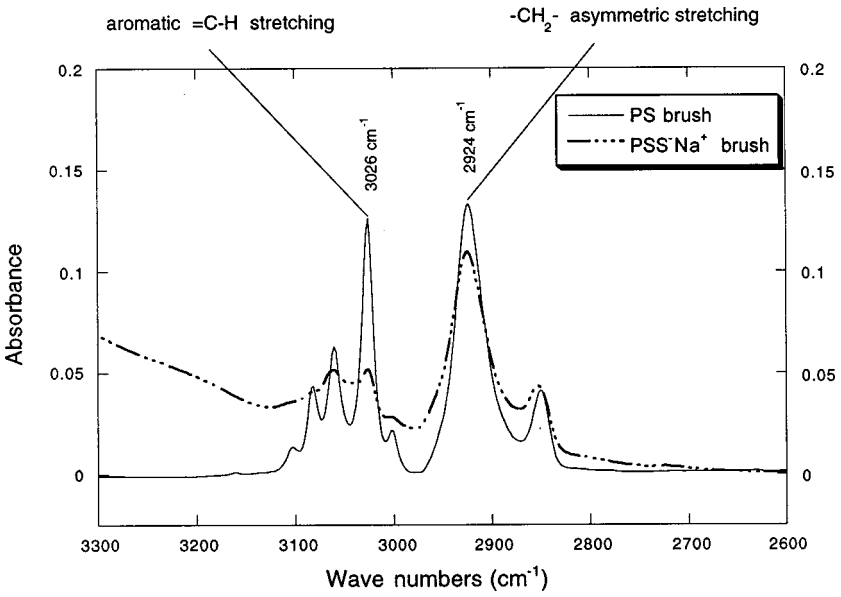

FIG. 2. IR-ATR spectrum of a PS brush before (solid line) and after (dashed dotted line) sulfonation.

ATR) and to determine the structure of the interfaces using neutron reflectivity. Both techniques are sensitive to H-D substitution, which allows one to focus on one particular component of the interface at a time (for instance, the backbone of the grafted chains or the counterions). The polystyrene chains were synthesized anionically and terminated at one end by a trichlorosilane group which can react with the oxide surface of the silicon blocks. The grafting reaction was performed as described in Ref. [17]. The thickness of the resulting grafted PS layer was measured by ellipsometry: this allowed us to determine the amount of polymer per unit area and to calibrate the IR-ATR technique. Indeed, from the thickness of the dry PS brush measured by ellipsometry, we can calculate the number of the $—CH_2—$ (and aromatic —CH—) groups per unit area. The same samples were characterized by IR-ATR; the absorbance at 2924 cm^{-1} (characteristic of the $—CH_2—$ group) and at 3026 cm^{-1} (characteristic of the aromatic —CH— group) was measured (cf. Fig. 2) and thus, combining the results of both techniques, calibration curves, ''absorbance versus number of $—CH_2—$ groups per unit area'' (respectively, aromatic —CH— groups per unit area), were obtained. The PS chains were then converted into poly(styrene sulfonic acid) by a soft sulfonation reaction adapted from Ref. [18]. Finally, the chains were neutralized with sodium bicarbonate or with a dilute tetraethylammonium hydroxyde solution. The sulfonation yield was determined by comparing the intensity of the aromatic —CH— group absorption band (at 3026 cm^{-1}) before and after sulfonation (cf. Fig. 2). This band is specific to a monosubstitution of the phenyl ring. The neutralization rate was estimated using deuterated PS chains and protonated tetraethylammonium hydroxide as base. Comparison of the absorbance at 3010 cm^{-1} (characteristic of the ethyl group) with bulk samples proved that the neutralization was complete in the polyelectrolyte brush. The homogeneity of the sulfonation along the backbone was also checked by using a block copolymer PS(D)-PS(H)$SiCl_3$ [number of D (respectively, *H*) monomers: 156 (respectively 131), polydispersity index = 1.03]. After sulfonation, the degree of substitution of each block was found equal to that of the corresponding homopolymer. More details about the synthesis and the characterization will be given in a forthcoming publication.

III. COUNTERION COMPLEXATION

We investigated the complexation of different counterions: small cations [mono or divalent, for instance, Na^+, Ca^{++}, $(CH_3)_4N^+$, $(C_2H_5)_4N^+$], model polycations [poly(benzyl vinyl pyridium) ($PBVP^+$)] as well as two different proteins. The $PBVP^+$ were obtained after quaternization of anionically synthetized poly(2-vinyl pyridine). The degree of quaternization was found to be 0.40 (from elementary analysis). The proteins (lysozyme, molecular weight $M_W = 14.3$ kg/mol, extracted from chicken egg white and fibrinogen, $M_W = 310$ kg/mol, from bovine plasma) were from Aldrich. Under physiological conditions, the lysozyme (respectively, the fibrinogen) has a net charge of $+8$ (respectively, -10). Starting from a PSS^-Na^+ brush, the Na^+ ions were substituted by a given counterion X^+ by immersing the initial brush in a solution of X^+. The immersion time was typically 1 h, and the concentration of the X^+ solution was $0.1M$ for the small counterions, $0.01M$ for the $PBVP^+$, and 0.01 g/l buffered at pH = 7.4 for the proteins. Kinetics experiments showed that the immersion time was long enough and the molarities high enough to ensure a ''complete'' exchange: no further change was observed at longer time and higher concentration. After rinsing the excess of free X^+ with water, the amount of complexed X^+ was measured by several methods: IR in ATR if X^+ had absorption bands which did not overlap with those of the PSS^- brush skeleton [this is the case, for instance, when $X^+ = (CH_3)_4N^+$ and deuterated PSS^- is used], ellipsometry (for $PBVP^+$ and proteins), and neutron reflectivity (see below). We are thus led to define two charge ratios, which will be especially useful for the discussion of the polycation complexation: the stoichiometric charge ratio $r_s(X^+)$, which is the ratio of the sulfonate groups effectively complexed by X^+ and the total number of sulfonate groups, and the global charge ratio $r_g(X^+)$, which is the ratio of the total number of positive charges due to X^+ bound to the brush (per unit area) and the number of brush sulfonates (per unit area). By definition,

$0 \leqslant r_s(X^+) \leqslant 1$, whereas $0 \leqslant r_g(X^+) < +\infty$ (because the number of positive charges due to X^+ trapped by the brush can exceed the number of sulfonate groups).

For each of the counterions, the reversibility of the complexation was examined by immersing the brush complexed by X^+ in a 0.1 M solution of either NaCl or $(CH_3)_4NCl$ for 1 h, followed by rinsing with pure water. The amount of X^+ which remained trapped by the brush was then measured. It turns out that all the small counterions are reversibly complexed to the brush: each of them can be readily replaced by another provided there is enough of the latter in solution. On the contrary, the polycations and proteins are irreversibly trapped by the brush. Increasing the molarity of the small ions (used for the exchange test)—up to 5*M*—or the immersion time—up to 24 h—did not change the results. Finally, we determined the stoichiometric charge ratio for the polycations in the following way: the brush (made of protonated PSS^-) complexed by a given $PBVP^+$ was immersed for 1 h in a 0.1*M* solution of $(CD_3)_4NCl$ and the amount of $(CD_3)_4N^+$ which remained trapped in the interfacial layer after rinsing was measured by IR-ATR. This gave us the number of SO_3^- groups (per unit area) which were not involved in the complexation with the polycation and by difference $r_s(PBVP^+)$. The same result was obtained if we started directly from a PSS^- $(CD_3)_4N^+$ brush and measured the remaining $(CD_3)_4N^+$ ions after complexation with the polycations.

IV. INTERFACIAL STRUCTURE AND COUNTERION DISTRIBUTION

The structure of the brush complexed by the different counterions described above was determined by neutron reflectivity, using silicon blocks as substrates (as for the IR-ATR experiments) and D_2O as solvent [19]. Neutron reflectivity is a technique well adapted to the study of planar interfaces [20–23]. In our case, the incoming neutron beam traversed the silicon block before reflecting at the silicon D_2O interface. Because neutrons are sensitive to H-D substitution, it was possible to look at either the brush skeleton or the counterions separately. In the first case, the brush was made from protonated poly(styrene sulfonate) with $(CD_3)_4N^+$ (or Na^+) as counterions, while in the second case, the brush skeleton was 96% deuterated (matching the scattering length density of D_2O) and the counterions protonated. The best fit density profile of the protonated species $\phi(z)$, z being the distance normal to the silicon D_2O interface, to the reflectivity curve, was obtained using standard procedures [20]. We have used the kinematic approximation which links the neutron reflectivity to the gradient of the scattering length density profile $Nb(z)$ by

$$R(k) = R_F(k) \left| \int_0^\infty \frac{dNb}{dz} \exp(2ikz)\, dz \right|^2, \qquad (1)$$

where k is the wave vector, $k = 4\pi \sin\theta/\lambda$, λ is the neutron wavelength, and θ the angle of incidence. The Fresnel reflectivity $R_F(k)$ is the reflectivity of the bare surface. We modeled $Nb(z)$ with a (fixed) number of layers of constant scattering length density, calculated the corresponding reflectivity curve using Eq. (1), and found the parameters which best fit the data. The adjustable parameters were the thickness h_i, the scattering length density Nb_i, and the roughness σ_i of the layer i. This roughness (of the error function type) allowed one to connect two adjacent layers in a smooth way. Thus,

$$Nb(z) = \sum_{n=0}^{N} \left(\frac{Nb_i - Nb_{i+1}}{2} \right) \left(1 - \mathrm{erf} \frac{(z - z_i)}{\sigma_i} \right),$$

with $h_i = z_i - z_{i+1}$. The $n = 0$ and $n = N$ ''layers'' are semi-infinite media ($Nb_{N+1} = 0$). We have $Nb_0 = 2.0273 \times 10^{-6}$ Å^{-2} (scattering length density of the silicon). It appeared that only four layers were enough to account for all our data. No significant improvement was obtained if we increased the number of layers up to 10. Among these layers, the first one ($n = 1$) describes the oxide layer, present at the surface of the silicon blocks. Its characteristics were determined before grafting and did not change afterwards. Thus, for all our samples, only nine adjustable parameters were needed to account for the contribution of the monomers (or the counterions) to the scattering length density profile. After the determination of these parameters, the last operation was to go from $Nb(z)$ back to $\phi(z)$. Usually, this is straightforward. However, in our case, it was necessary to take into account the presence of some H_2O which was strongly bound to the PSS chains during the preparation of the polyelectrolyte brushes. The presence of such H_2O molecules which could not be replaced by D_2O was detected by other methods (IR-ATR and x-ray). Thus the 96% deuterated brush, which in principle is contrast matched with D_2O, gave rise to a signal that was (slightly) different from the expected Fresnel reflectivity. Nevertheless, it turns out that the volume fraction of this trapped H_2O was the same for all the samples ($\approx$25%). These water molecules probably solvate the sulfonate groups. If we assume that these H_2O molecules are distributed throughout the polymer layer in the same way as the sulfonates (or the counterions), then $\phi(z)$ can be obtained as

$$\phi(z) = \frac{Nb_{D_2O} - Nb(z)}{(Nb_{D_2O} - Nb_M) + w(Nb_{D_2O} - Nb_{H_2O})}, \qquad (2)$$

where Nb_M is the scattering density of the protonated species (either PSSNa or the counterions). w is the amount of trapped H_2O. w was precisely determined by comparing $\gamma = \int_0^\infty \phi(z)\, dz$ with the layer thickness measured by ellipsometry (which is the total amount of matter in the interface per unit area).

A typical result is given in Fig. 3. It shows the reflectivity curve of a poly(styrene sulfonate sodium salt) brush in D_2O. Its main characteristics are as follows: polymerization index $N = 310$ (polydispersity = 1.04), distance between two grafting sites $D = 21$ Å, and sulfonation rate $\alpha = 0.45 \pm 0.10$. The solid line is the best fit to the data, corresponding to the density profile shown in Fig. 4 (dash-dotted line). The concentration profile appears to decrease slowly and extends far into the bulk. The typical thickness of this charged brush is more than 2 times greater than the typical thickness of the corresponding neutral brush in good solvent (PS brush, with the same number of monomers and the same

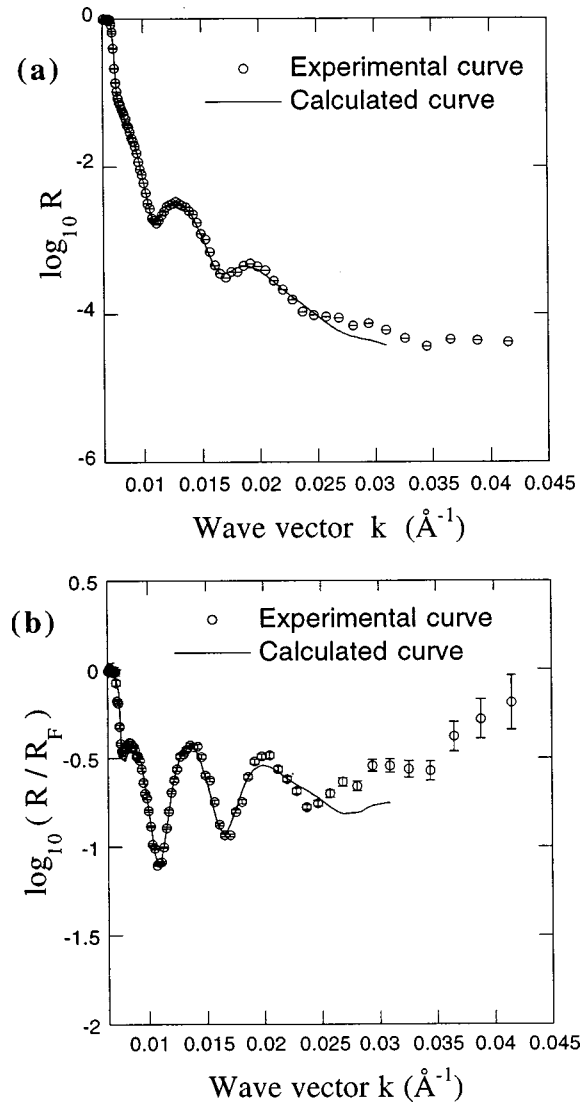

FIG. 3. Reflectivity curve of a protonated PSSNa brush in D_2O. The solid line is the best fit to the data corresponding to the volume fraction profile shown in Fig. 4 (dash-dotted line). Two representations are displayed: reflectivity $\log_{10}[R(k)]$ vs k in (a) and $\log_{10}(R/R_f)$ vs k in (b), which emphasizes the contribution of the polymer volume fraction profile to the reflectivity.

grafting density). We also observed that the chain extension is proportional to the chain length and does not depend on the grafting density. These results characterize the osmotic regime which has been predicted [1,9,10] for highly charged dense polyelectrolyte brushes. In this regime, the chains can be viewed as if they each were stretched by the osmotic pressure due to their own counterions. This means that all the counterions should be confined inside the brush, ensuring a highly local electroneutrality. This physical picture can be tested by determining the counterion distribution.

The density profile of tetramethylammonium counterions is shown in Fig. 4. The poly(styrene sulfonate) brush was 96% deuterated to render it ''invisible'' in neutron reflectivity; its characteristics ($N=300$, $D=21.9$ Å, $\alpha=0.40 \pm 0.10$) are comparable to those of the protonated brush. In Fig. 4, the $(CH_3)_4N^+$ density profile has been normalized to account for the difference in molecular volume between styrene sulfonate and tetramethylammonium. This makes possible a direct comparison of the density profiles in terms of charge distribution. We observe that the counterion distribution follows quite closely the backbone monomer distribution; this means that within the brush, the electroneutrality is very local. The counterions are confined inside the polyelectrolyte interface and exert a strong osmotic pressure which induces the chain stretching.

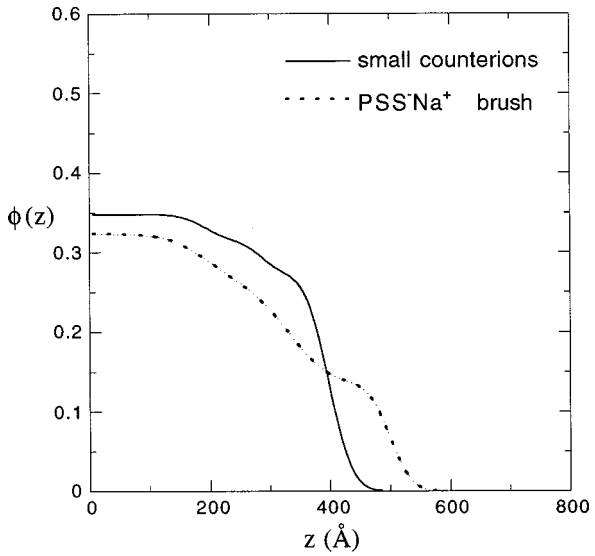

FIG. 4. Interfacial distribution of small counterions (tetramethylammonium) compared to the interfacial structure of a poly(styrene sulfonate sodium salt) brush. $\phi(z)$ is the volume fraction as a function of distance z (Å) from the surface.

The results obtained with macromolecular counterions ($PBVP^+$) are totally different. First, we remind the reader that the complexation of these polycations is irreversible: they cannot be replaced by small ions. Second, in contrast to the small counterions which are distributed across the entire brush, the polycations are localized in the external region of the brush. This segregation is more pronounced with increasing polycation chain length (see Fig. 5). The addition of salt into the bulk (up to $5M$) does not modify these results. The backbone density profile (which was not determined) might be also affected by the presence of the complexed polycations. Indeed, one can imagine that the polycations might induce a contraction of the outer border of the brush (which is the less dense part), leading to a more pronounced segregation. Nevertheless, the external localization of the polycations would result from a compromise between electrostatic energy, which promotes penetration of the positively charged chains into the negatively charged brush, and the chain elasticity and polymer incompatibility (both of entropic nature) which are unfavorable to polymer association. This scheme would account for the effect of the polycation length. Another type of explanation which could also be invoked might be the glassy state of the dense brush near the solid surface. It would allow the exchange of small ions, but not the deep penetration of polycations, which are much bigger objects. Therefore, the external localization of $PBVP^+$ would be the result of a kinetic barrier. It is difficult to discriminate between the two interpretations; however, we never observed an increase of the complexed $PBVP^+$ amount, even after several days of incubation. This would support the first interpretation (in terms of thermodynamic

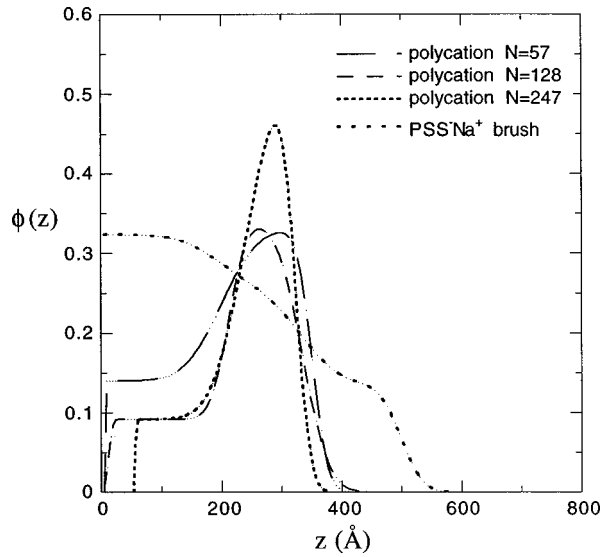

FIG. 5. Interfacial distribution of polycations ($PBVP^+$ of three different lengths) compared to the interfacial structure of the same poly(styrene sulfonate sodium salt) brush as in Fig. 4.

equilibrium). Theoretical studies and computer simulations could help in this discussion.

Whatever the explanation, the question of the inner brush sulfonates in the presence of the complexed polycations must be addressed: did they keep their (small) initial counterions? Indeed, the external localization of the $PBVP^+$ suggests that some of these sulfonates would not be involved in the complexation with the polycations. Moreover, we can calculate (from the neutron reflectivity and the ellipsometry data) that, as a whole, there are only 0.4 pyridinium groups per sulfonate monomer [$r_g(PBVP^+) \approx 0.4$]. To answer this question, we measured the stoichiometric charge ratio $r_s(PBVP^+)$ by allowing the (possible) Na^+ counterions to exchange with $(CD_3)_4N^+$, as explained above. We found that $r_s(PBVP^+, N=57) = 0.40 \pm 0.11$ (40% of the brush sulfonates are complexed with pyridinium groups of the smallest $PBVP^+$), and for the two longer polycations, $r_s(PBVP^+, N=128$ or $N=247) = 0 \pm 0.12$. Less than 12% of the sulfonate groups are involved in the complexation of the ''long'' polycations. Likewise, the fraction of pyridinium effectively bound to sulfonates (which is equal to r_s/r_g) is very small; most of the charged monomers keep their small counterion. However, it has to be noted that the error bar on r_s/r_g is rather large ($\approx 30\%$).

The fact that only a small fraction of the polycation monomers might be involved in the complexation as soon as the chains are long ($N \geqslant 100$) would not be in contradiction with the irreversibility of the complexation. Indeed the energy cost to replace a monomer by a small ion might be small (compared to the thermal energy—kT), but because each of the polycation chains is bound by several links, the total energy might far exceed kT and, as a result, the complexed chains cannot be displaced by small ions. This effect is well known for conventional adsorbed polymers.

We also investigated the possibility of building multilayers starting with our polyelectrolyte brushes. It was observed that after complexation of $PBVP^+$, no additional layer of free poly(styrene-sulfonate–sodium-salt) could be adsorbed.

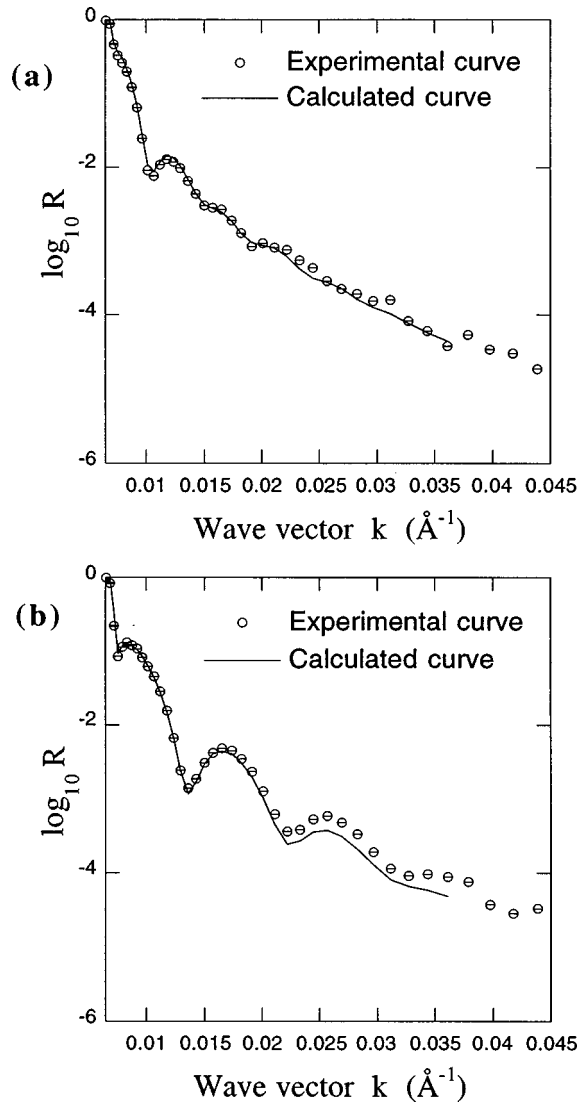

FIG. 6. Reflectivity curves of (a) fibrinogen and (b) lysozyme adsorbed on a deuterated brush, in D_2O. Characteristics of the brush: $N=300$, $D=21.9$ Å, $\alpha = 0.40 \pm 0.10$.

This indicates that despite their external localization, the complexed $PBVP^+$ chains are not able to invert the surface charge of the polymer layer: at the outer border of the polymer layer, there must be some PSS^- chains which are not overcompensated by $PBVP^+$; therefore, they would prevent the adsorption of other free polyanions. This contrasts with the results of Refs. [7,8], which showed that multilayers can be obtained with adsorbed PSS^- and poly(methylvinylpyridinium)-$PMVP^+$. In their case, the global charge ratio $r_g(PMVP^+)$ was found to be 3, whereas it is only 0.4 for our PSS^- brush/$PBVP^+$ complex. This difference is certainly related to the dense grafting of the PSS^- chains, which strongly restricts the polymer conformations. The grafted polyanions cannot adapt their conformation to accommodate as much polycation as the electrostatic interaction would allow.

It appears that the brush complexed with $PBVP^+$ prevents further adsorption of either PSS^- or $PBVP^+$. It would be interesting to extend this investigation to other polyanions and polycations to assess the generality of this interesting antiadsorption property.

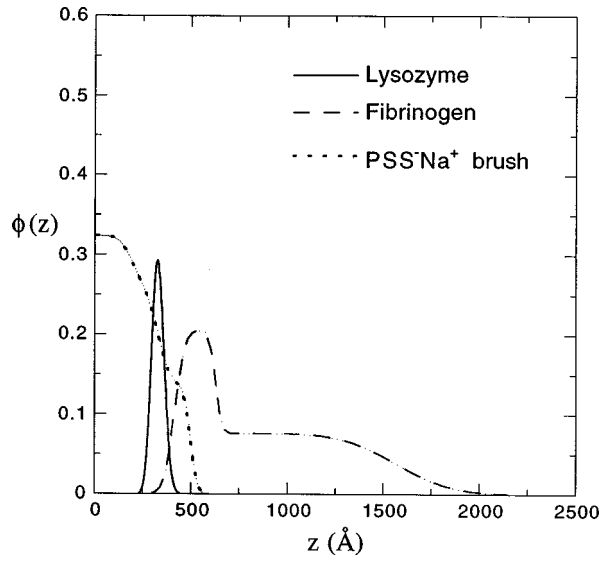

FIG. 7. Interfacial distribution of proteins under physiological conditions (pH$=7.4$) compared to the interfacial structure of the same poly(styrene sulfonate sodium salt) brush as in Fig. 4. The adsorbed amount of lysozyme (respectively, fibrinogen) is 3.5 mg/m^2 (respectively, 15.8 mg/m^2).

Finally, we also looked at the interaction between the brush and two different proteins: lysozyme and fibrinogen. Both adsorb strongly onto the brush: they cannot be removed by small ions. Both are also located nearly outside the grafted polyelectrolyte layer (cf. Figs. 6 and 7); they are kept away from the (solid) surface by the brush. This is a direct proof that such dense charged polymer layers can efficiently protect a surface from the approach of macromolecular objects, but at the same time can be permeable to small molecules. It is worthwhile to discuss in more detail the shape of the protein density profiles. Lysozyme, which carries a net positive charge of $+8$, has about the same number of monomers as the medium size PBVP$^+$. Its density profile, however, is different: it has a symmetrical bell shape, without any ''tail'' reaching the surface. This suggests that the adsorbed lysozymes are not denaturated, but keep their native ellipsoidal shape of $45\,\text{Å}\times 30\,\text{Å}\times 30\,\text{Å}$ in size. The adsorbed lysozyme layer (of maximum volume fraction ≈ 0.3) could thus be modeled as a nearly half-filled layer of protein clusters. These aggregates would contain three to four proteins in order to match the thickness of the layer ($\approx$200 Å). Fibrinogen, on the other hand, has a quite different density profile. On the basis of its net charge (-10, under physiological conditions), this protein is not expected to adsorb onto the brush. But it is well known that fibrinogen has specific binding sites for sulfate or sulfonate groups, which play an important role in blood coagulation. Indeed, fibrinogen, under the action of thrombin, is converted into fibrin and this latter protein can form a network which is the basic ingredient of a blood clot. This sequence of events does not occur in the presence of heparin, a sulfate-rich polysaccharide, because heparin strongly binds to fibrinogen and inhibits the action of thrombin. The adsorption of fibrinogen onto the poly(styrene-sulfonate–sodium-salt) brush would thus be mediated by the (positively charged) binding sites for sulfate (or sulfonate); this would correspond to the more dense layer in direct contact with the brush. The other part of the density profile (the dilute tail extending very far into the bulk) would correspond to the rest of the protein, which is negatively charged and therefore strongly repelled by the brush. Compared to the native shape of the protein (an elongated ellipsoid of $450\,\text{Å}\times 60\,\text{Å}\times 60\,\text{Å}$ in size), the density profile of the adsorbed fibrinogen suggests that this protein is quite severely denaturated by the adsorption on the brush.

V. CONCLUSION AND OUTLOOK

Dense polyelectrolyte brushes allow exchanges of small counterions. Macromolecular counterions, as well as some proteins, are irreversibly trapped, but they adsorb only at the outer border of the brush. They are kept away from the surface; this emphasizes the protective role that these brushes can play. In addition, when macromolecular counterions are bound to the brush, the polymer complex layer exhibits some promising antiadsorption properties. The methodology used in this study, which combines IR-ATR spectroscopy and neutron reflectivity, could be used to address other challenging questions; for instance, it might be possible to directly ''view'' the action of a restriction enzyme onto an adsorbed protein.

[1] P. Pincus, Macromolecules **24**, 2912 (1991).
[2] A. G. Moat and J. W. Foster, *Microbial Physiology*, 3d ed. (Wiley-Liss, New York, 1995).
[3] E. Pefferkorn, A. Carroy, and R. Varoqui, Macromolecules **18**, 2252 (1985).
[4] E. Pefferkorn, Adv. Colloid Interface Sci. **56**, 33 (1995).
[5] J. Papenhuyzen, G. J. Fleer, and B. H. Bijsterbosch, J. Colloid Interface Sci. **104**, 530 (1985).
[6] J. Marra, H. A. Van der Schee, G. J. Fleer, and J. Lyklema, in *Adsorption from Solution*, edited by R. Ottewill, C. H. Rochester, and A. L. Smith (Academic, New York, 1983).
[7] Gero Decher, Science **277**, 1232 (1997) and references therein.
[8] N. G. Hoogeveen, M. A. Cohen-Stuart, and G. J. Fleer, Langmuir **12**, 3675 (1996).
[9] J. Wittmer and J. F. Joanny, Macromolecules **26**, 2691 (1993).
[10] O. V. Borisov, E. B. Zhulina, and T. M. Birshtein, Macromolecules **27**, 4795 (1994) and references therein.
[11] J. L. Harden, Macromolecules **30**, 5930 (1997) and references therein.
[12] C. Amiel, M. Sikka, J. W. Schneider, Y. H. Tsao, M. Tirrell, and J. W. Mays, Macromolecules **28**, 3125 (1995).
[13] P. Guenoun, A. Schalchli, D. Sentenac, J. W. Mays, and J. J. Benattar, Phys. Rev. Lett. **74**, 3628 (1995).
[14] Y. Mir, P. Auroy, and L. Auvray, Phys. Rev. Lett. **75**, 1863 (1995).
[15] H. Walter, G. Harrats, P. Müller-Buschbaum, R. Jérôme, and M. Stamm, Langmuir **15**, 1260 (1999).
[16] M. Biesalski and J. Rühe, Macromolecules **32**, 2309 (1999).
[17] O. Ou Ramdane, P. Auroy, and P. Silberzan, Phys. Rev. Lett. **80**, 5141 (1998).

[18] H. S. Makowski, R. D. Lundberg, and G. S. Singhal, U.S. Patent No. 3870841 (1975).

[19] The neutron reflectivity experiments were done at the Laboratoire Léon Brillouin (France) and at the Royal Appleton Laboratory–ISIS Facility (UK). We thank J. Webster for his assistance. The experiments done at RAL were supported by the European Union through its TMR Program for Large Scale Facilities.

[20] T. P. Russell, Mater. Sci. Rep. **5**, 171 (1990); M. S. Kent, L. T. Lee, B. J. Factor, F. Rondelez, and G. S. Smith, J. Chem. Phys. **103**, 2320 (1995).

[21] G. Fragneto, R. K. Thomas, A. R. Rennie, and J. Penfold, Science **267**, 657 (1995) and references therein.

[22] T. J. Su, J. R. Lu, R. K. Thomas, Z. F. Cui, and J. Penfold, Langmuir **14**, 438 (1998).

[23] M. Stamm, in *Scattering in Polymeric and Colloidal Systems*, edited by K. Mortenson and W. Brown (Gordon and Breach, New York, 1999).